Chapter 3

On the Theory of the CO+OH Reaction: Tunneling Effect and the O-isotope Anomaly

[This chapter submitted to the *Journal of Chemical Physics*.]

Abstract

The kinetic oxygen isotope effect (KIE) in the HO+CO reaction is different from the value expected in the Bigeleisen-Mayer formula. The possible factors influencing the small KIE in $H^{18}O$+CO are discussed. Since these factors can differ in their sign, the calculation results are sensitive to the theoretical input. Qualitative features are described for comparing with the experimental results. An experiment that avoids a possible role of vibrationally excited OH radicals as reactants is also suggested. The effect of H-tunneling on the well-known Bigeleisen-Mayer formula for the KIE is also discussed. The results reduce to the expected from that B-M result when the tunneling is omitted.

I. INTRODUCTION

The $CO+OH \rightarrow CO_2+H$ reaction is known to be the principal reaction for oxidizing CO in the atmosphere and controlling the OH radical concentration.[1] It has been extensively studied both by experiments[2–16] and by theoretical calculations.[16–24] Our own interest in the reaction from: it having been occasionally identified as a reaction showing a "mass-independent" oxygen isotope fraction. This result appeared strange since it is unlike ozone fractionation that has a symmetry effect and whose mass-independent fractionation (MIF) has this origin. We shall see that, in fact, a three-isotope plot points to an isotopic anomaly rather than an MIF.

In our previous papers,[25,26] many experimental observations, including the pressure and temperature dependence of the reaction rate constants, and the H- and C-isotope effects, were treated using the RRKM theory and a nonstatistical modification and agreed with the experimental data. Previous evidence for a nonstatistical behavior of the reverse reaction at higher energies was seen in the molecular beam experiments of Simons and coworkers[27,28] Experimentally there is an anomalous oxygen kinetic isotope effect (KIE),[29,30] anomalous in the sense of not obeying the Bigeleisen-Mayer rule.[31,32] The present study was undertaken to explore this issue, as well as to study another aspects of the Bigeleisen-Mayer rule, namely the effect of molecular tunneling, here of H and D.

The currently accepted mechanism for the reaction is that an OH radical reacts with CO, producing a vibrationally excited energetic *trans*-HOCO*.[4,12,15,16,20,21] This step is followed by *cis-trans* isomerization, and the final competitive steps are the dissociation to

H and CO_2, the back reaction to OH and CO, and a collisional stabilization of HOCO*. When the pressure is increased, collisional stabilization of the energetic HOCO* competes increasingly favorably with the forward dissociation channel and the back reaction. When OH and CO react in air or oxygen, both the dissociation channel and collision stabilization lead to the same products, HO_2 and CO_2, due to the follow-up reactions of the H and HOCO with O_2.[33–35]

A theoretical treatment of the oxygen KIE has not been given previously. Kurylo and Laufer appear to be the first group who used heavy oxygen isotopes to study the reaction experimentally.[36] They produced ^{18}OH radicals photochemically photolyzing $H_2{}^{18}O$ with 184.9 nm radiation, then leaving them reacting with CO in a static cell. They reported that $C^{18}O$ was produced at low pressure, and disappeared in the presence of 760 torr of SF_6, suggesting that there was isotopic exchange between the $C^{16}O$ and the ^{18}OH, but did not report a rate constant. Using a thermal source of ^{18}OH, namely from H atoms reacting with NO_2 or F atoms reacting with H_2O in a flow tube, Greenblatt and Howard[37] did not observe a measurable isotopic exchange and concluded that the rate constant for the isotopic exchange of ^{18}OH with $C^{16}O$ was no larger than 10^{-15} cm^3 molecule^{-1} s^{-1}. Thus, there are two different observations of the O-exchange although it has been suggested by the latter group that other reactions on the walls of the static cell may have caused the exchange in the Kurylo and Laufer study.[37] However, the issue has not yet been resolved in the literature. Whereas these two groups of authors studied isotopic exchange, Stevens and co-workers used mass spectroscopy and, importantly, used a photolytic source of OH radicals to study the oxygen KIE in $C^{18}O$.[29] They measured the

isotopic ratios of the unreacted CO, and obtained pressure-dependent enrichment of the $^{18}O/^{16}O$ ratio over the pressure range of 150 to 800 torr.

Later experimental studies of the heavy oxygen KIE using $C^{18}O$, were made by Röckmann et al. using a photolytic source of OH radicals[30] and by Feilberg et al. using photolytic ozone reacting with water to form OH radicals.[38] The pressure-dependent fractionation results of ^{18}O by Röckmann et al. are comparable to those by Stevens et al., but differ from those of Feilberg et al.[38] The precursors generating the OH radicals differed in the two studies. The experimental conditions by Röckmann et al. are simpler, in that no ozone is added and many fewer chemical reactions contribute to the overall reaction scheme. While HO_2 may be a dominant product in the studies of Röckmann et al.[30] and Stevens et al.[29] due to the reaction of the source material H_2O_2 with OH and in principle could have interfered, the rate constant for the reaction of CO with HO_2 is extremely small, about 10^{-27} cm^3 molecule^{-1} s^{-1} at room temperature.[39] Thus, it is about 14 orders of magnitude smaller than that of CO with OH and would not interfere in the studies in references 29 and 30.

The anomalous oxygen KIE in the CO+OH reaction is examined in the present work. Our calculated result shows that the KIE in this reaction is a compromise between two opposing effects: (1) a heavy isotope favors the formation of TS_2 (the transition state from HOCO* to CO_2+H) due to an increase the number of states of a transition state relative to the partition of reactants, and (2) a light isotope (^{12}C and ^{16}O) favors the formation of TS_2 because of the reduced imaginary frequency in the tunneling reaction coordinate. The present article discusses the dominance of these two effects in various

isotopomers. The calculation result shows that the carbon KIE is dominated qualitatively by the former and the oxygen KIE at CO by the latter.

The article is organized as follows: The calculational methods are outlined in section II. The results are given in section III and discussed in section IV.

II. CALCULATIONAL METHODS

The calculational methods are the same as those described previously,[25,26] and are briefly summarized here. At any energy E and total angular momentum J, we have

$$\mathrm{CO} + \mathrm{OH} \underset{k_{-1}(EJ)}{\overset{k_1(EJ)}{\rightleftharpoons}} \mathrm{HOCO}^*(EJ), \tag{1}$$

$$\mathrm{HOCO}^*(EJ) \overset{k_2(EJ)}{\longrightarrow} \mathrm{H} + \mathrm{CO_2}. \tag{2}$$

The transition states for reactions (1) and (2) are abbreviated as TS_1 and TS_2, respectively. In the kinetic scheme, the density of states of the energetic intermediate HOCO* includes density of states of the both *cis*-HOCO* and *trans*-HOCO*, since the rotational barrier for *cis-trans* conversion is far lower than the energy of reactants and a rapid conversion can be assumed. At finite pressures an additional series of kinetic equations is added:

$$\mathrm{HOCO}^*(EJ) + \mathrm{M} \overset{\omega(EJ \to E'J')}{\longrightarrow} \mathrm{HOCO}(E'J') + \mathrm{M}, \tag{3}$$

where M is a third body. The total rotational-vibrational energy E and the total angular momentum J are conserved in reaction steps (1) and (2). The rate constants are all E- and J-dependent; $\omega(EJ \to E'J')$ is the rate constant per unit E for forming HOCO at $(E'J')$ from (EJ) by collision with a third body M. The collision frequency

$\omega(EJ \rightarrow E'J')$ is factored approximately into the total collision frequency ω, the energy transfer probability $P_{E \rightarrow E'}$, and the rotational angular momentum transfer probability $P_{J \rightarrow J'}$. Thereby, the energy transfer probability is $\omega(EJ \rightarrow E'J') = \omega P_{E \rightarrow E'} P_{J \rightarrow J'}$. $P_{E \rightarrow E'}$ is approximated by a stepladder model,[40,41] in which a certain amount of energy α is transferred between the intermediate HOCO* and a bath molecule in each collision. Because of the smallness of the C and O isotope effect, it is necessary to use a fine division of energies. The use of the stepladder instead of a continuous model in this treatment of very small isotope effects saves a factor of 10 in computational time and resources, as discussed in reference 41. The α value is taken as dependent on the bath gas but independent of pressure and isotopic substitution in HOCO. The α values of various bath gases were obtained in our previous paper by best fit to the experimental data.[25] For angular momentum transfer a strong collision was assumed. Thereby, the transfer probability $P_{J \rightarrow J'}$ equals the thermal distribution of rotational states of the intermediate HOCO*, at the given temperature,[40] i.e., $P_{J \rightarrow J'} = (2J'+1)\exp(-B_J[J'(J'+1)-J(J+1)]/k_BT)/(2J+1)$, where B_J is the rotational constant of J.

The rate constants of the CO+OH reaction were calculated as a function of pressure by solving the rate equations for reactions (1)–(3) using microcanonical RRKM calculations. Tunnelling corrections for both TS_1 and TS_2, and a steady-state equation for pressure effects were included. The H-tunneling correction was estimated from a transmission through an Eckart potential[42] passing through the saddle-point. (For the given *ab initio* potential energy surfaces the TS_2 lies in the exit channel, and so there is little or no "corner cutting.") At room temperature the tunneling at TS_1 contributes about 20%

of the total rate constant.[25] An *ab initio* potential energy for the important equilibrium structures was calculated by Lin and co-workers,[20] who used the modified Gaussian-2 method (G2M). To obtain the more accurate vibrational frequencies and rotational constants for all equilibrium structures for the various isotopes we used, as before,[25,26] a coupled-cluster method,[43,44] abbreviated as CC.[45] The optimized structures and vibrational frequencies of all stationary structures are given in Table I of reference 25. In our earlier work,[25] the potential energy of TS_1 and TS_2 were shifted vertically slightly by two independent constants to match the experimental rate constants with the non-Arrhenius effect at low temperature and the energy transfer parameters used to described the pressure effect at room temperature in various bath gases. We made no further change here.

The above results are compared in appendix A with another potential energy surface for all stationary structures (LTSH by Schatz and co-workers[23,46]). The robustness was tested using other methods, as discussed in appendix A.

III. RESULTS

A. Slopes of the Three-Isotope Plot and "Mass-Independent" Fractionation

Apparently not mentioned before in the isotope reaction-rate literature is the effect of H-tunneling on the well-known three-isotope plot and the Bigeleisen-Mayer laws.[31,32] The enrichment or depletion is defined as

$$\delta \mathrm{Q} \equiv \left(\frac{(\mathrm{Q}/^{16}\mathrm{O})_{\mathrm{sample}}}{(\mathrm{Q}/^{16}\mathrm{O})_{\mathrm{standard}}} - 1 \right) \times 1000 \text{ per mil}, \tag{4}$$

where the "Q" in the equations denotes ^{17}O or ^{18}O. A plot of $\delta^{17}O$ vs $\delta^{18}O$ constitutes the well known three-isotope plot for O isotopes. According to the usual "mass-dependent" theory of Bigeleisen and Mayer,[31,32] the slope is about 0.52 for oxygen isotopes, a result well established in the experimental literature for systems with no mass-anomaly. A MIF has been defined in two ways. A technically rigorous definition is a slope of unity for the 3-isotope $\delta^{17}O$ vs $\delta^{18}O$ plot ("mass-independent"). In a second definition the deviation from mass-dependence often used is when a $\Delta^{17}O$ defined in equation (5) differs from zero:

$$\Delta^{17}O \equiv \delta^{17}O - 0.52 \times \delta^{18}O \neq 0. \tag{5}$$

The $\Delta^{17}O$ is popularly used since it requires only a pair of ($\delta^{17}O$, $\delta^{18}O$) measurements, whereas a 3-isotope plot requires a whole series of measurements.

Two fractionation properties for the KIE of oxygen, εCQ and εHQ, can be defined, according as the heavy oxygen is in the CO or in the OH:

$$\varepsilon CQ \equiv \left(\frac{k_{CO+OH}}{k_{CQ+OH}} - 1\right) \times 1000 \text{ per mil}; \tag{6}$$

$$\varepsilon HQ \equiv \left(\frac{k_{CO+OH}}{k_{CO+QH}} - 1\right) \times 1000 \text{ per mil}. \tag{7}$$

In a kinetic-controlled reaction with a small amount of reaction, the enrichment defined in equations (6) and (7) approximately equals the fractionation defined in equation (4), i.e., $\varepsilon CQ \cong \delta CQ$ and $\varepsilon HQ \cong \delta HQ$. The experimental and calculated slopes of the three-isotope plots in the present study are listed in Table I, together with the range of fractionations $\Delta^{17}O$ of the CQ+OH reaction in two bath gases, He and N_2, at total pressures below 1000 torr. The slope of $\varepsilon H^{17}O$ vs $\varepsilon H^{18}O$ in He obtained by RRKM the-

TABLE I: Calculated and experimental slopes of the three-isotopes plots and range of Δ^{17}Os in He or N_2 at pressures between 0 and 1000 torr[a]

	RRKM (no tunneling)	RRKM	Nonstatistical	Expt.[30]
		He		
$\varepsilon C^{17}O$ vs $\varepsilon C^{18}O$	0.45	0.39	0.39	1.1[b]
$\varepsilon H^{17}O$ vs $\varepsilon H^{18}O$	0.52	0.56	0.56	—
Δ_{CQ}	0.13 to 0.75	0.20 to 0.92	0.29 to 0.98	2.3 to 3.0[b]
Δ_{QH}	1.58 to 2.11	−0.79 to −1.11	−0.96 to −1.25	—
		N_2		
$\varepsilon C^{17}O$ vs $\varepsilon C^{18}O$	—	0.36	0.36	1.6[c]
$\varepsilon H^{17}O$ vs $\varepsilon H^{18}O$	—	0.60	0.58	—
Δ_{CQ}	—	0.20 to 1.02	0.27 to 1.07	2.8 to 4.5[c]
Δ_{QH}	—	−0.80 to −1.22	−0.97 to −1.39	—

[a]The R-squared values of the linear fits are better than 0.95. The units are per mil.

[b]There are only two experimental points at 188 and 525 torr.

[c]The bath gas is N_2 or N_2+O_2. The pressures are at 188, 375, and 660 torr.

ory without including tunneling has the usual mass-dependent value, as seen in Table I. All other slopes of the fractionation show an "anomalous" mass effect, i.e., they differ from the Bigeleisen and Mayer rule. The calculated εHQ is larger than the εCQ. The deviation of the experimental result from the Bigeleisen-Mayer rule is consistent with the importance of H-tunneling in TS_2. The importance of TS_2 at low pressure supported by the H/D effect.

B. KIE for Oxygen

Only the εCQ values have been measured experimentally thus far. The $\varepsilon C^{18}O$ values in Fig. 1 calculated by the RRKM method and by a nonstatistical modification are about +4 and +3 per mil, respectively, at low pressure. As the pressure is increased, the values calculated by both models decrease monotonically to around −2 per mil at 1000 torr (Fig. 1). The calculated pressure dependence of the ^{18}O KIE in different bath gases (N_2 and He) is very similar. The robustness of the calculated ^{18}O values is seen in appendix A. All the calculated results made with the different *ab initio* methods give similar $\varepsilon C^{18}O$ values, all positive and 5 to 7 per mil, at low pressure. We consider in section IV C a qualitative explanation for the sign of this result rather than focusing on small differences in quantitative. The agreement largely rests on one key assumption; the same argument explaining why the KIE of ^{18}O and ^{13}C have opposite signs at low pressure (The possible reasons are given in appendix B.).

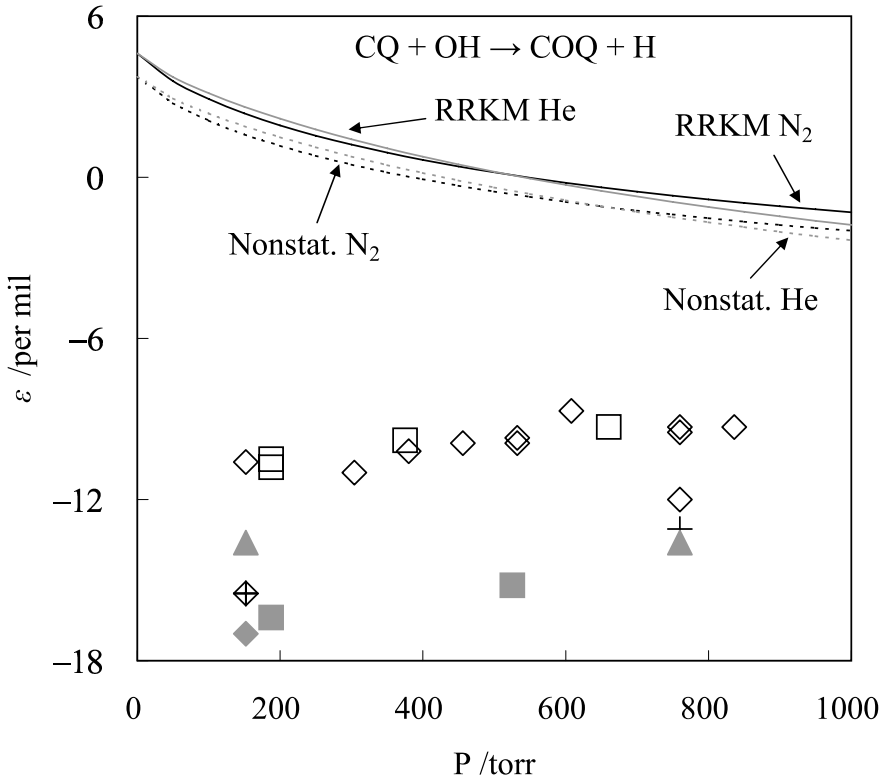

FIG. 1: $\varepsilon C^{18}O$ calculated using the RRKM method and the nonstatistical model for the OH+CO reaction as a function of total pressure. The data given by gray closed and black open squares were obtained in He (or Ar), and N_2 (or N_2+O_2), respectively, by Röckmann.[30] and by Stevens.[29]

IV. DISCUSSION

A. Mass-Dependent Effect and the Three-Isotope Plot

According to Bigeleisen's and Mayer's "mass-dependent" rule,[31,32] the expected slope of a three-isotope plot of oxygen isotopes is ∼0.52. When the reaction is either a single step or consists of a preequilibrium followed by a rate determining step in the absence of H-tunneling, the usual mass-dependent Bigeleisen-Mayer isotope behavior is expected to occur. However, when there are competitive processes in a mechanism or when there is nuclear tunneling, there is no requirement that the slope have this value. The calculated slopes of $\varepsilon C^{17}O$ vs $\varepsilon C^{18}O$ and $\varepsilon H^{17}O$ vs $\varepsilon H^{18}O$ at various pressures in Table I without H-tunneling effect are seen to have smaller deviations from 0.52 than those with tunneling. The large tunneling effect in the dissociation reaction (2) thus introduces a larger anomalous mass effect in the CO+OH reaction. Such potential sources of breakdown of the rule for mass-dependent behavior, tunneling or complexity of mechanism, do not appear to have been mentioned in the literature.

The magnitude of the fractionation $\Delta^{17}O$, equation (5), is sometimes used to identify a "mass-independent" effect in reactions. However, $\Delta^{17}O$ can differ from zero for a variety of reasons, some having nothing to do with the mass-independent effect seen in ozone, as noted earlier. In Table I the calculated Δ_{OH} using RRKM without tunneling has incidentally the largest value, even though the corresponding slope in the three-isotope plot is 0.52, the "ideal" value of mass-dependent slope for the oxygen isotopes. Hence, the magnitude of $\Delta^{17}O$ appears here in the intercept of the plot. Using only

$\Delta^{17}O$ as a criterion for a "mass-independent fractionation" is convenient, but does not distinguish among alternative sources of the deviation, H-tunneling and complexity of mechanism, and is different from the current (symmetry-based) molecular basis of the mass-independent effect. In fact, even when $\Delta^{17}O$ is appreciable in Table I, the slope of the three-isotope plot can still be far from the real *mass-independent* value of unity. As a generic term, values of $\Delta^{17}O$ different from zero can be termed "*mass-anomalous,*" rather than a special class of which–those with unit slope–"*mass-independent.*"

B. The Major Facts in the KIE

The enrichment of the ^{13}C and ^{18}O at low pressure is the result of two opposing effects, as mentioned earlier and as we now elaborate on: (1) the heavy isotope tends to increase the number of states at the transition states relative to the thermally averaged partition function of the reactants and so favors the heavier isotope; (2) the tunneling through transition states favors the lighter isotope, because of its greater participation in the H-dominated tunneling coordinate. To assess the relative importance of these two factors for any set of computations, we consider also the case where transition state TS_2 is regarded as rate controlling but where tunneling is neglected. In that case only the first factor is present and the enrichment is seen in Table II to be negative. When tunneling is included, the participation of heavier oxygen isotopes in the tunneling coordinate favors the positive enrichment of the lighter oxygen isotopes in the products. However, the carbon atom is able to form more bonds with the surrounding atoms. Since the heavier carbon reduces the vibrational and rotational constants, it causes a favor of the heavier

TABLE II: Comparison between calculated RRKM fractionation with and without tunneling in the low-pressure limit[a]

	Without Tunnelling[b]	With Tunnelling
$C^{17}O$+OH	−2.30	2.60
$C^{18}O$+OH	−5.54	4.62
CO+^{17}OH	−24.62	8.58
CO+^{18}OH	−50.38	18.32
^{13}CO+OH	−59.25	−3.97

[a]Units are in per mil.

[b]There are few changes of the enrichment values as the barrier of TS_2 is lowered by 340 cm^{-1}. It shows that the enrichment is insensitive to the exact value of barrier high as long as the TS_2 is the rate-determining step.

carbon isotopomer in the reaction constant at low pressure.

C. Sources for the Oxygen KIE

To analyze the theoretically calculated $C^{18}O$ KIE, we are focusing on zero pressure, since the physical interpretation is the most transparent there. The essence of the result for the ^{18}O KIE at zero pressure is seen using the following ratio that appears in the integral over E and J for the zero-pressure rate constant:

$$k_{\text{rate}}(EJ) = \frac{k_1 k_2}{k_{-1} + k_2} = \frac{N_1 N_2}{Q(N_1 + N_2)} e^{-E/k_B T}. \tag{8}$$

The variables N_1 and N_2 are the number of states of TS_1 and TS_2, respectively; and Q is the partition function for the reactants' collision pair in the center of mass system. The expression has the form of an effective number of TS states, $1/N_{eff} = 1/N_1 + 1/N_2$, a "sum of resistances." The potential energy of TS_1 and TS_2 were constrained by the non-Arrhenius behavior in a wide temperature range (83–3300 K). As discussed in reference 25, the rate constant at high temperatures is dominated by the barrier of TS_2. At room temperature the calculated thermally weighted $N_1 \simeq 3.8 N_2$.[47] Thus, in equation (8) the ratio of $N_1/(N_1 + N_2)$ is roughly unity, and then the low pressure limit of the rate constant of the reaction is given approximately by

$$k_{N_2}^{\text{approx}} = \int_E \mathrm{d}E \sum_J \frac{N_2}{Q} e^{-E/k_B T}, \tag{9}$$

and so is dominated by TS_2, in which tunneling plays an important role, as discussed in the above section. The importance of TS_2 is seen in the H/D isotope effect at room

temperature, which tends to a value slightly greater than 3 as the pressure tends to zero. (Theory and experiments discussed in reference 25.)

Table III it is shown that the calculated ε for ^{18}O is similar to the $\varepsilon_2^{\text{approx}}$. (The definition of the latter is similar to equations (6) and (7) but using the ratio of $k_{N_2}^{\text{approx}}$s for the two isotopomers.) Because of the dominant calculated role of N_2 in contributing to the rate constant, the calculated sign of $\varepsilon C^{18}O$ reflects primarily the effect of the heavier mass in reducing the effective tunneling mass at TS_2. It reduces the tunneling frequencies in TS_2 and hence reduces the rate constant, thus causing a positive values of the calculated $\varepsilon C^{18}O$ at low pressure in Fig. 1. Because all masses in the HOCO* contribute to the effective tunneling mass, the products tend to be enriched in the lighter isotope. Calculations in appendix C illustrate the robustness of the calculated result, a robustness understood if the key hypothesis is valid, namely that TS_2 is rate controlling at low pressure and room temperature. If H/D tunneling were unimportant then the calculated isotope effect would be of opposite sign, as shown in Table II.

D. Comparison of Experiments and Calculations

In both Stevens's and Röckmann's independent measurements,[29,30] the $\varepsilon C^{18}O$ values in He, Ar, or O_2 are about -15 per mil, while those in N_2 or air are about -10 per mil, as seen in Fig. 1. The pressure dependence of the $\varepsilon C^{18}O$s is seen there to be minor. The experimental ΔCQ values obtained by Röckmann et al. are about 2.5 per mil at 200 torr and increase to about 3 per mil at 500 torr in He and to about 4.5 per mil at 900 torr in N_2. In an application to atmospheric problems, the effect of such an enrichment

TABLE III: Comparison between calculated fractionation $\varepsilon_1^{\text{approx}}$, $\varepsilon_2^{\text{approx}}$ and ε in the low-pressure limit[a]

	$\varepsilon_1^{\text{approx}}$	$\varepsilon_2^{\text{approx}}$	ε
^{13}CO+OH	16.33	−10.24	−3.97
C^{17}O+OH	1.50	3.35	2.60
C^{18}O+OH	−0.77	7.17	4.62
CO+^{17}OH	14.34	8.51	8.58
CO+^{18}OH	33.20	17.35	18.32

[a]Units are in per mil.

on the seasonal fractionation changes in the oxygen isotopes of the atmospheric carbon monoxide was discussed in reference 30. The calculated Δ_{CQ} values are in the range 0.2–1.1 per mil, as seen in Table I, which is slightly smaller than experimental values, 2.3–3.0 per mil.

In our calculations using both the RRKM and the nonstatistical models, the results for the calculated $\varepsilon C^{18}O$ values are offset from the experimental values by about +15 per mil, as seen in Fig. 1. As discussed in the above section and in the additional information in appendix C, the compact structure of TS_2 leads a well-defined transition state and to a calculated $\varepsilon C^{18}O$ at low pressure that is dominated by TS_2 and is positive. This calculational result is different from experiment. A possible origin of this discrepancy is discussed in the section IV E. Although the sign of $\varepsilon C^{18}O$ in low-pressure limit are different in calculation and experiments, both calculated and experimental of $\varepsilon C^{18}O$ show minor pressure dependence as pressure is varied from 0 to 1000 torr, as seen in Fig. 1.

E. A Possible Explanation of the $^{16}O/^{18}O$ Discrepancies and a Proposed Experiment

One possible explanation of this $^{16}O/^{18}O$ discrepancy is in the theory. Another possibility is that this discrepancy in the $\varepsilon C^{18}O$ in the CO+OH reaction is experimental, due to a nonthermal effect. In particular the OH radicals in the experiments in references 29 and 30 are formed photochemically and if they are vibrationally hot, the mass dependence of heavier oxygen isotopes in CO in the reaction would be affected, since intramolecular H-transfer reaction in the energetic HOCO* may occur. This isotope exchange effect

would not change the mass dependence of carbon isotopes, and so our previous work that reproduced the sign and pressure dependence of latter would be unaffected.[25] It would also be consistent with the experiments in reference 36.

When the HOCO* has a large excess energy, an isotopic exchange of the oxygen atoms between CO and OH in the vibrationally excited HOCO* molecule becomes possible. This reorganization can reform the reactants without forming products. Two possibilities for the intramolecular H-transfer are:

$$\textit{trans}\text{-HOCQ}^* \longrightarrow \text{HCO}_2 \longrightarrow \textit{trans}\text{-OCQH}^*, \tag{10}$$

$$\textit{cis}\text{-HOCQ}^* \longrightarrow \textit{cis}\text{-OCQH}^*. \tag{11}$$

In reaction (10) the intermediate HCO_2 has the hydrogen atom close to the carbon atom instead of an oxygen atom, but might occur by "roaming." Reaction (10) recalls the new "roaming" H-atom mechanism seen in the photodissociation of formaldehyde.[48–50] Although when zero-point energy is not included reaction (10) had a shallow well, calculated as 840 cm^{-1}, but the zero-point energy of HCO_2 makes the effective well disappear.[20] Reaction (11) is a direct intramolecular H-transfer reaction from one oxygen atom to the other, possible for the *cis* geometry but not for the *trans*.

The calculated geometries and vibrational frequencies of the structures in reactions (10) and (11) are listed in Table IV. In our *ab initio* CC calculations, relative to the separated reactants, the barrier of reaction (10) without zero-point corrections is about 3500 cm^{-1}, and that of reaction (11) is more than 8000 cm^{-1}, so only reaction (10) needs to be considered in an intramolecular mechanism. The barrier in reaction (10)

TABLE IV: CC-calculated geometries and vibrational frequencies of the transition structures of normal isotopes in Reactions (10) and (11)[a]

	Reaction (10)	Reaction (11)
R_{OH}	1.242	1.337
R_{CO}	1.318	1.266
R_{CQ}	1.191	1.266
θ_{HOC}	61.30	68.25
θ_{OCQ}	142.69	116.35
d_{HOCQ}	180.0	0.0
ν_1	$1952i$	$2257i$
ν_2	496	840
ν_3	666	1049
ν_4	1147	1328
ν_5	1862	1658
ν_6	2233	2044

[a]The units are in Å for bond length, in degree for angles and dihedral angles, and in cm^{-1} for vibrational frequencies.

has a large value of the imaginary frequency with H-transfer, and so both tunneling and dynamic effects would be important when the internal energy of HOCO* is high enough for reaction (10) to occur. When thermalized OH radicals at room temperature are used, the calculated rate constant for forming HCO_2 is less than 10^{-17} cm^3 molecule^{-1} s^{-1}, reaction (10) would contribute only about 0.1 per mil to the ε of the CO+OH reaction so be negligible.

In the experiments of Kurylo and Laufer,[36] oxygen isotopic exchange of OH and CO was reported in the depleted reactants at low pressure. Due to the photolysis used to generate OH radicals, some of the radicals may be vibrationally hot when they react later with CO. Since HOCO* is now at a higher energy, the reaction rate of the intramolecular hydrogen exchange, reaction (10), could be enhanced. This presumption is consistent with Kurylo and Laufer's observation,[36] which implies H-transfer reaction involving in the CO+OH reaction at low pressure. In contrast to Kurylo and Laufer's experiment, there was no observable H-transfer reaction in Greenblatt and Howard's study,[37] but in the latter the OH radicals were generated by chemical reactions rather than by photolysis.

The OH radicals in both Stevens's and Röckmann's experiments were generate by photolysis of H_2O_2 with an Hg or Xe lamp,[29,30] so the resulting OH radicals may have excess vibrational energy. Even if the excess energy results in the reaction rates of hydrogen transfer of only about 1.5% of the rate of the ordinary CO+OH reaction, namely has a rate constant of 2×10^{-15} to 3×10^{-15} cm^3 molecule^{-1} s^{-1}, it would decrease the $\varepsilon C^{18}O$ values in the present calculations to values nearly the same as those in the experimental results, and would also change the Δ_{CO} value to about 7 per mil,

and so be of the same order as the experimental value. Thus, new measurements of the $\varepsilon C^{18}O$ and Δ_{CO} using a thermalized source of OH could offer useful insight into this issue and also resolve the difference between the experiments of Stevens and Röckmann on one hand and those of Kurylo and Laufer on the other.

F. Oxygen KIE in QH

Using a spectroscopic detection of OH, Greenblatt and Howard measured rate coefficients for the reaction of ^{18}OH and ^{16}OH with CO to be $(1.49 \pm 0.15) \times 10^{-13}$ and $(1.44 \pm 0.15) \times 10^{-13}$ cm^3 molecule^{-1} s^{-1}, respectively.[37] This kind of measurement of absolute rather than relative values of the rate constants for the different isotopes gives too large an error to compare with the present calculations. However, using mass-spectroscopy, such as in Stevens's and Röckmann's measurements,[29,30] the accuracy of measuring KIE is sufficient to determine the oxygen isotope effect.

Although the KIE in QH is not the main focus of this paper does not appear in the literature yet, we compare it with the KIE in CQ. The reduction in the imaginary frequency due to heavier oxygen leads to a decreased tunneling. The effect is seen in Table V to be greater when the heavier oxygen is in OH than when it is in CO, a result qualitatively expected because the O in OH is closer to the H in HOCO* than when it is in CO, and so contributes more dynamically to the effective tunneling mass. Accordingly the calculated εHQ is larger than the calculated εCQ at all pressures, a result seen in both the RRKM and the nonstatistical models, as seen in Fig. 2. The effect of the imaginary frequency of TS_2 dominating the difference between εHQ and εCQ is also

TABLE V: Calculated imaginary frequency of TS_2 by CC for different oxygen isotopes[a]

	H···OCQ	H···QCO
Q = ^{16}O	2126i	2126i
Q = ^{17}O	2125i	2116i
Q = ^{18}O	2123i	2107i

[a]The units are cm^{-1}.

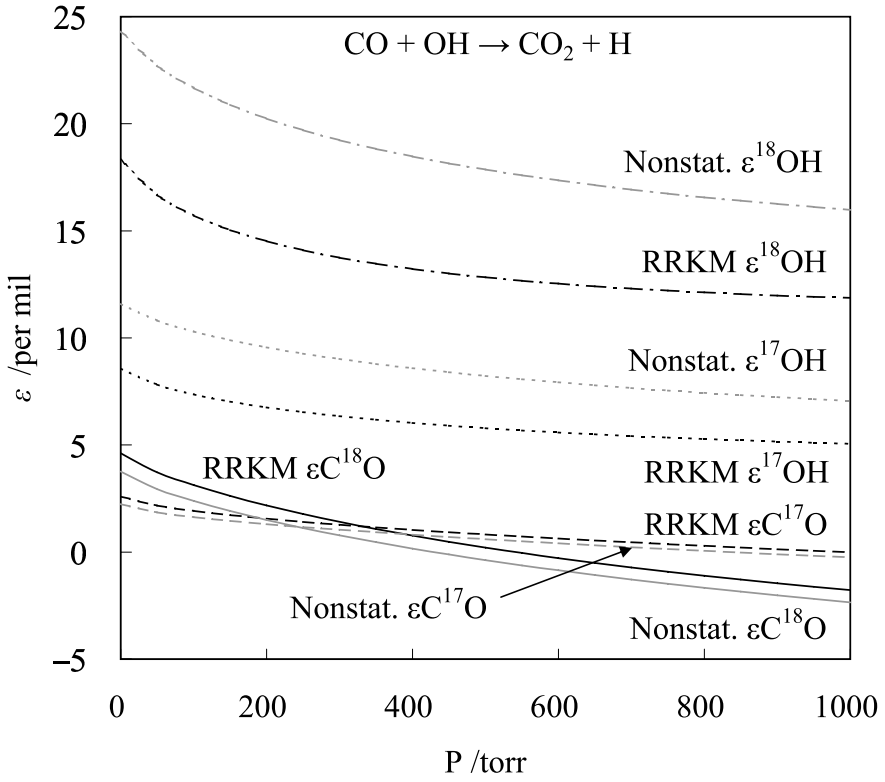

FIG. 2: Pressure dependence of the calculated εCQ and εHQ values for the OH+CO reaction. The black and gray lines are obtained using the RRKM method and the nonstatistical model, respectively. Since both N_2 and He bath gases give similar results, only the calculations with N_2 are shown in the plot.

seen in the calculations made with other *ab initio* methods (Appendices). Therefore, using thermalized source of QH could be helpful in comparing with this prediction and so testing further the importance of the H-tunneling effect in the reaction.

V. CONCLUSIONS

The mass-independent character in a reaction is better defined by the slope in a three-isotope plot, instead the magnitude of fractionation, Δ, since a reaction such as CO+OH may have peculiar mass-dependence with nonzero Δ value. The CO+OH reaction is better described as a mass-anomalous reaction, instead of mass-independent. Since it involves an energetic HOCO intermediate without a preequilibrium followed by a rate-determinate step, the slope in a three-isotope plot is expected to be different from the ideal mass-dependent value, $\sim$0.52.

Its oxygen KIE is a compromise between two opposing effect: (1) a heavy isotope tends to increase the ratio between the number of state at transition states and the thermally average partition function of reactants; (2) a light isotope tends to increase the tunneling effect at transition states. Their importance in the reaction at room temperature and at pressures below 1000 torr was studied with RRKM theory and with a nonstatistical modification, both including and excluding the nuclear tunneling of H at the TSs, using a potential energy surface and the parameters that are the same as those used previously.[25] The reaction in the current calculation favors lighter oxygen isotope since tunneling dominates the calculated fractionation, which is different in the heavier carbon isotopomer. The different dominated effect between the carbon and oxygen KIE

is qualitatively explained by the bond-order properties in these two elements. Although the same treatment as that given in our previous paper[25] reproduced a large body of experimental data discussed there, there is a discrepancy between the measured and calculated anomalous mass dependence of oxygen isotopes in the reaction. The calculated sign of ^{18}O enrichments at low pressure and room temperature rests on only one key assumption, namely that the TS_2 with tunneling dominate TS_1.

The discrepancy for oxygen from experiments may instead be due to an intramolecular hydrogen transfer reaction (10) arising from vibrationally hot OH radicals. This hypothesis can be tested by measuring the O-isotope effect using thermalized OH radicals, perhaps such as those used in the work of Greenblatt and Howard.[37] Since the OH radicals in Stevens's and in Röckmann's experiments were produced by photolysis,[29,30] the OH radicals may have had excess vibrational energy, introducing the possibility of the intramolecular H-atom transfer "roaming" reaction (10), with an immediate consequence for the O-isotope effect discussed in Section IV E. Using thermalized OH radicals to study the kinetic oxygen isotope effects would eliminate such a high-energy mechanism and so be an appropriate for testing the present theory regarding the dominance of TS_2 at low pressure and room temperature.

Acknowledgments

It is a pleasure to acknowledge the support of this research by the National Science Foundation. We also thank Dr. Muckerman for providing the F matrix for the structures in their paper,[17] which were used to check the accuracy of rate-constant calculation with

our previous vibrational frequencies.

APPENDIX A: CALCULATED RESULTS FOR DIFFERENT PES'S

The robustness of the results of the present calculations was explored using other electronic structure methods. In particular, to test the sensitivity of certain aspects of the calculations, different, albeit less accurate, methods were used. They are discussed in this appendix. Apart from the transition state structure of the entrance channel TS_1,[51] the vibrational frequencies and rotational constants of all structures for the various isotopes were calculated by three methods, CCSD(T) with 6-31G(d,p), B3LYP with cc-pVTZ, and MP2 with 6-31++G(d,p). The properties of TS_1 are obtained only from the results of MP2 or CC, since DFT gives an unrealistic structure.[51] The acronym DFT denotes the calculation by B3LYP, DFT-MP denotes the calculations combining the structure data of TS_1 from MP2 and the structures from B3LYP, while DFT-CC is similar but with the data for TS_1 obtained from CCSD(T). The GAUSSIAN 98 program[52] was employed for all three *ab initio* calculations (CC, MP2, and B3LYP) to obtain the principal equilibrium structures and their rotational and vibrational constants.

With the force constants and rotational constants at the same *ab initio* level, both G2M and LTSH potentials give very similar calculated results for the oxygen isotope effect. At the low pressure limit at room temperature, the calculated $\varepsilon C^{18}O$ values are about 6, 7, 5, and 2 per mil for DFT-CC, DFT-MP, CC, and MP2, respectively, with G2M or LTSH potentials. The RRKM and nonstatistical modification give similar results. In the pressure range from 0 to 1000 torr the values for all PESs except MP2 are

greater than -2 per mil, as shown in Fig. 3. The imaginary frequency of TS_2 by MP2 is unreasonably large, $3176i$, and so gives lower calculated values of $\varepsilon C^{18}O$, monotonically decreasing from 2 to -6 per mil as the pressure changes from 0 to 1000 torr. Because of the unreasonable OH frequency in MP2, the MP2 results are omitted in Fig. 3.

The calculated fractionation for the oxygen atom in OH, $\varepsilon H^{18}O$ at low pressure is again positive and is about 4, 11, 18, and 39 per mil with force constants obtained by using DFT-CC, DFT-MP, CC, and MP2, respectively. The large difference in $\varepsilon H^{18}O$ and $\varepsilon C^{18}O$ is similar to the trend of the values of the imaginary frequency in TS_2 obtained for various calculational levels.[53] This trend is also similar to the trend of the difference between $\varepsilon H^{18}O$ and $\varepsilon C^{18}O$ at low pressure.

APPENDIX B: COMPARISON OF O AND C KIE

Compared oxygen KIE with the carbon's in reference 25, both calculation and experiments shows that the $\varepsilon^{13}CO$ values have a larger pressure dependence than $\varepsilon C^{18}O$ when the pressure is varied from 0 to 1000 torr. At low pressure limit, the $\varepsilon^{13}CO$ value is negative, as discussed in the above two sections, because the TS_2 still dominates the reaction and the heavier isotope decreases the vibrational and rotational constants, its number of states in ^{13}C increases more than that in normal isotope, shown in Table III. Although reducing tunneling effect due to ^{13}C also contributes to reducing the number of states in TS_2, similar to that in heavier oxygen isotope, increasing number of states of TS_2 by reducing vibrational and rotational constants dominates in the ^{13}C isotopomer. The dominance effect in number of states in ^{13}C is different from that in heavy oxygen

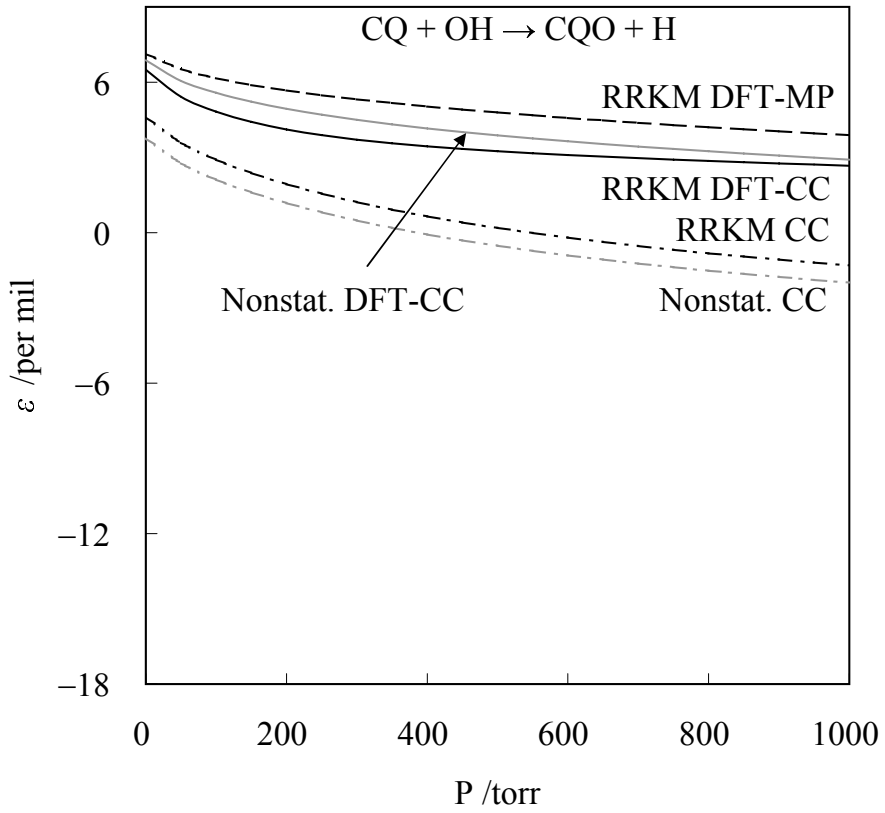

FIG. 3: Calculated $\varepsilon C^{18}O$ values for the OH+CO reaction as a function of total pressure. The G2M and LTSH potentials and He and N_2 bath gases all give results similar to those plotted, namely the results with G2M in N_2 are shown in the plot. The black and gray lines are obtained with the RRKM method and the nonstatistical model, respectively. The solid, dashed-dot, and dashed lines are calculated with DFT-CC, CC, and DFT-MP, respectively. (The reason for not showing MP2 results is given in appendix A.)

isotopomers because the carbon atom can form more bond with surrounding atoms than oxygen atom. This crucial difference leads to the different fractionation behavior at low pressure limit in our present calculation.

As the discussion in our previous article of the non-Arrhenius behavior,[25] the barrier of TS_2 dominates rate constants at high temperature regions, and both barriers contribute rate constants at low temperature regions. Although the usual KIE is smaller at higher temperature, due to the non-Arrhenius behavior the absolute value of the calculated $\varepsilon C^{18}O$ and $\varepsilon^{13}CO$ at low pressure limit show that as increasing temperature, instead of monotonic decreasing in the usual KIE, they reach a maximum at ∼400 K, as seen in Table VI.

Another parameter is introduced here to show the robustness in the fractionation at low pressure limit, especially the oxygen KIE. Since TS_2 involves dissociation of a hydrogen atom from HOCO*, the imaginary frequencies is difficult to obtain precisely using *ab initio* methods.[20,25] The imaginary frequency of TS_2 is scaled by a factor. Using the same fitting procedures of the two vertical shifted parameters of TS_1 and TS_2 described in reference 25, The scaling factor to best represent the calculated pressure dependence of carbon KIE, as shown in Fig. 4, is 0.95 and 0.85 for RRKM and nonstatistical modification, respectively. Although changing the value of imaginary frequency has some improvements on the carbon KIE, Table VII shows that the scaling factor has negligible effect on the oxygen KIE. This result is expected since, as discussed in section IV C and shown in Table III, both $\varepsilon_1^{\text{approx}}$ and $\varepsilon_2^{\text{approx}}$ have contribution on the carbon fractionation, but the oxygen fractionation is mainly dominated by $\varepsilon_2^{\text{approx}}$ in our present calculation.

TABLE VI: Temperature dependence of $\varepsilon C^{18}O$ and $\varepsilon^{13}CO$ at low-pressure limit [a]

	$\varepsilon C^{18}O$	$\varepsilon^{13}CO$
200 K	1.29	0.89
298 K	4.62	−3.97
400 K	5.38	−4.94
500 K	5.28	−4.53
600 K	4.87	−3.56

[a]Units are in per mil.

TABLE VII: $\varepsilon C^{18}O$ and $\varepsilon^{13}CO$ at low pressure limit [a]

	Scaling Factor[b]	$\varepsilon^{13}CO$	$\varepsilon C^{18}O$
RRKM	1.00	−3.97	4.62
RRKM	0.95	−5.47	4.43
Nonstatistical	1.00	−0.18	3.76
Nonstatistical	0.85	−3.67	3.62

[a]Units of fractionation are in per mil.

[b]A scaling factor of the imaginary frequency of TS_2, see text.

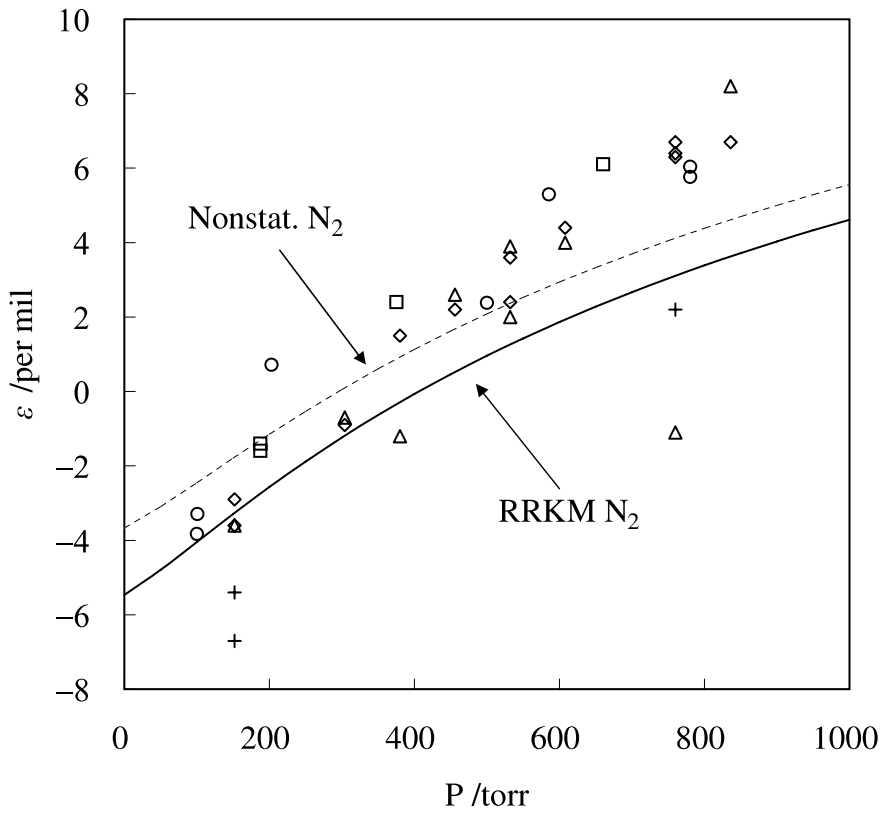

FIG. 4: The ε^{13}CO values for the system of CO+OH given as a function of total pressure at room temperature. The solid lines are calculated using the conventional RRKM theory with a scaling factor 0.95 on the imaginary frequency of TS_2, and the dashed line is obtained with the nonstatistical model with a similar scaling factor, but with value 0.85. Open circles are obtained for N_2 by Smit et al.[54] Black open squares are obtained in N_2 or N_2+O_2, respectively, by Röckmann.[30] Black open triangle, open diamond, and plus symbols are obtained in Ar, air (by measuring products), air, and O_2, respectively, by Grose.[55]

APPENDIX C: CALCULATED $\varepsilon_1^{\text{approx}}$, $\varepsilon_2^{\text{approx}}$, AND ε

The definition of $\varepsilon_1^{\text{approx}}$ is similar to that of $\varepsilon_2^{\text{approx}}$ but with a $k_{N_1}^{\text{approx}}$ similar to $k_{N_2}^{\text{approx}}$ in equation (9), with N_1 instead of N_2 in the integral. At zero pressure, the calculated $\varepsilon_1^{\text{approx}}$, $\varepsilon_2^{\text{approx}}$, and ε of different *ab initio* methods are given in Table VIII. The ε value shifts from $\varepsilon_2^{\text{approx}}$ toward $\varepsilon_1^{\text{approx}}$ when the ratio of thermally weighted N_1 and N_2 decreases. Even with an unreasonably large value of the imaginary frequency in MP2, which gives nearly equal contributions to KIE from both TS_1 and TS_2, the calculated $\varepsilon C^{18}O$ is still positive at zero pressure. Thus, the different methods as well as the argument based on equation (9) yield positive ε values, in contrast to current experiment.

TABLE VIII: Calculated N_1/N_2, $\varepsilon_1^{\text{approx}}$, $\varepsilon_2^{\text{approx}}$, and ε at low pressure limit of different *ab initio* methods[a]

	N_1/N_2[b]	$\varepsilon_1^{\text{approx}}$	$\varepsilon_2^{\text{approx}}$	ε
		CC		
$C^{17}O$+OH	3.80	1.50	3.35	2.60
$C^{18}O$+OH	3.82	−0.77	7.17	4.62
CO+^{17}OH	3.77	14.34	8.51	8.58
CO+^{18}OH	3.73	33.20	17.35	18.32
		DFT-CC		
$C^{17}O$+OH	5.75	2.68	3.96	4.04
$C^{18}O$+OH	5.77	2.66	7.05	6.49
CO+^{17}OH	5.64	16.35	−1.94	2.20
CO+^{18}OH	5.54	31.19	−4.79	3.62
		DFT-MP		
$C^{17}O$+OH	2.72	2.19	3.95	3.82
$C^{18}O$+OH	2.73	4.15	7.02	7.13
CO+^{17}OH	2.67	16.52	−2.07	5.67
CO+^{18}OH	2.62	34.69	−5.03	11.21
		MP2		
$C^{17}O$+OH	1.07	−0.10	3.31	1.31
$C^{18}O$+OH	1.08	−2.37	5.22	1.61
CO+^{17}OH	1.08	17.18	21.77	19.72
CO+^{18}OH	1.08	33.15	41.85	38.65

[a]The units of $\varepsilon_1^{\text{approx}}$, $\varepsilon_2^{\text{approx}}$, and ε are in per mil.

[b]The ratios of thermally weighted N_1 and N_2 at room temperature is listed in the N_1/N_2 column.

[1] R. P. Wayne, *Chemistry of Atmospheres* (New York: Oxford University Press, 2000), 3rd ed.

[2] A. Miyoshi, H. Matsui, and N. Washida, *J. Chem. Phys.* **100**, 3532 (1994).

[3] C. D. Jonah, W. A. Mulac, and P. Zeglinski, *J. Phys. Chem.* **88**, 4100 (1984).

[4] D. Fulle, H. F. Hamann, H. Hippler, and J. Troe, *J. Chem. Phys.* **105**, 983 (1996).

[5] A. R. Ravishankara and R. L. Thompson, *Chem. Phys. Lett.* **99**, 377 (1983).

[6] V. Lissianski, H. Yang, Z. Qin, M. R. Mueller, and K. S. Shin, *Chem. Phys. Lett.* **240**, 57 (1995).

[7] M. S. Wooldridge, R. K. Hanson, and C. T. Bowman, *Int. J. Chem. Kinet.* **28**, 361 (1996).

[8] M. S. Wooldridge, R. K. Hanson, and C. T. Bowman, in *25th Symp. (Intl.) Combust.* (1994), pp. 741–748.

[9] T. A. Brabbs, F. E. Belles, and R. S. Brokaw, in *13th Symp. (Intl.) Combust.* (1971), pp. 129–136.

[10] M. J. Frost, P. Sharkey, and I. W. M. Smith, *J. Phys. Chem.* **97**, 12254 (1993).

[11] M. J. Frost, P. Sharkey, and I. W. M. Smith, *Faraday Discuss. Chem. Soc.* **91**, 305 (1991).

[12] A. J. Hynes, P. H. Wine, and A. R. Ravishankara, *J. Geophys. Res.* **91**, 11815 (1986).

[13] A. Hofzumahaus and F. Stuhl, *Ber. Bunsenges. Phys. Chem.* **88**, 557 (1984).

[14] R. Forster, M. Frost, D. Fulle, H. F. Hamann, H. Hippler, A. Schlepegrell, and J. Troe, *J. Chem. Phys.* **103**, 2949 (1995).

[15] N. F. Scherer, C. Sipes, R. B. Bernstein, and A. H. Zewail, *J. Chem. Phys.* **92**, 5239 (1990).

[16] D. M. Golden, G. P. Smith, A. B. McEwen, C. L. Yu, B. Eiteneer, M. Frenklach, G. L. Vaghjiani, A. R. Ravishankara, and F. P. Tully, *J. Phys. Chem. A* **102**, 8598 (1998).

[17] H. G. Yu, J. T. Muckerman, and T. J. Sears, *Chem. Phys. Lett.* **349**, 547 (2001).

[18] T. V. Duncan and C. E. Miller, *J. Chem. Phys.* **113**, 5138 (2000).

[19] R. Valero and G. J. Kroes, *J. Chem. Phys.* **117**, 8736 (2002).

[20] R. S. Zhu, E. G. W. Diau, M. C. Lin, and A. M. Mebel, *J. Phys. Chem. A* **105**, 11249 (2001).

[21] J. P. Senosiain, C. B. Musgrave, and D. M. Golden, *Int. J. Chem. Kinet.* **35**, 464 (2003).

[22] R. Valero, D. A. McCormack, and G. J. Kroes, *J. Chem. Phys.* **120**, 4263 (2004).

[23] M. J. Lakin, D. Troya, G. C. Schatz, and L. B. Harding, *J. Chem. Phys.* **119**, 5848 (2003).

[24] D. M. Medvedev, S. K. Gray, E. M. Goldfield, M. J. Lakin, D. Troya, and G. C. Schatz, *J. Chem. Phys.* **120**, 1231 (2004).

[25] W. C. Chen and R. A. Marcus, *J. Chem. Phys.* **123**, 094307 (2005).

[26] W. C. Chen and R. A. Marcus, *J. Chem. Phys.* **124**, 024306 (2006).

[27] M. Brouard, D. W. Hughes, K. S. Kalogerakis, and J. P. Simons, *J. Chem. Phys.* **112**, 4557 (2000).

[28] M. Brouard, I. Burak, D. W. Hughes, K. S. Kalogerakis, J. P. Simons, and V. Stavros, *J. Chem. Phys.* **113**, 3173 (2000).

[29] C. M. Stevens, L. Kaplan, R. Gorse, S. Durkee, M. Compton, S. Cohen, and K. Bielling, *Int. J. Chem. Kinet.* **12**, 935 (1980).

[30] T. Röckmann, C. A. M. Brenninkmeijer, G. Saueressig, P. Bergamaschi, J. N. Crowley, H. Fischer, and P. J. Crutzen, *Science* **281**, 544 (1998).

[31] J. Bigeleisen and M. G. Mayer, *J. Chem. Phys.* **15**, 261 (1947).

[32] J. Bigeleisen, M. G. Mayer, P. C. Stevenson, and J. Turkevich, *J. Chem. Phys.* **16**, 442 (1948).

[33] J. T. Petty, J. A. Harrison, and C. B. Moore, *J. Phys. Chem.* **97**, 11194 (1993).

[34] J. Nolte, J. Grussdorf, E. Temps, and H. G. Wagner, *Z. Naturforsch. A: Phys. Sci.* **48**, 1234 (1993).

[35] G. Poggi and J. S. Francisco, *J. Chem. Phys.* **120**, 5073 (2004).

[36] M. J. Kurylo and A. H. Laufer, *J. Chem. Phys.* **70**, 2032 (1979).

[37] G. D. Greenblatt and C. J. Howard, *J. Phys. Chem.* **93**, 1035 (1989).

[38] K. L. Feilberg, S. R. Sellevag, C. J. Nielsen, D. W. T. Griffith, and M. S. Johnson, *Phys. Chem. Chem. Phys.* **4**, 4687 (2002).

[39] D. H. Volman, *J. Photochem. Photobiol. A-Chem.* **100**, 1 (1996).

[40] Y. Q. Gao and R. A. Marcus, *J. Chem. Phys.* **114**, 9807 (2001).

[41] Although there are other methods treating for collisional energy transfer, such as the exponential-down model, a stepladder model is computationally less intensive for the current purpose of treating small isotope effects. Since the difference of vibrational frequencies and rotational constants between isotopomers are small, the energy grain size for either model needs to be small enough to distinguish the difference between isotopomers. The energy grain size is 1 cm^{-1} in the current work to cover the 8000 cm^{-1} in the E range.[25] Using a

stepladder model with a typical energy transfer parameter α ($\sim$200 cm^{-1}), there are 200 40×40 square matrices to be solved in the master equation. However, in the test calculation the energy grain size for the exponential-down model to reach similar accuracy is around 5 cm^{-1}, requiring, thereby, a single 1600×1600 matrix in the master equation. Although the step-down model needs to have 200 matrices and the exponential-down model has only one, the size of matrix in the exponential down model is considerably larger than those in the stepladder model. Thereby, the stepladder model needed about one order of magnitude less computational resources than the exponential-down model. Test calculations showed that as long as the energy grain size is small enough to describe the properties of isotopomers, both models gave similar pressure dependence for the fractionation. The fractionation at low pressure is, of course, independent of the deactivation model.

[42] C. Eckart, *Phys. Rev.* **35**, 1303 (1930).

[43] The vibrational frequencies and rotational constants of all stationary structures are calculated by the CCSD(T) method with the 6-31G(d,p) basis set.

[44] The difference of rotational constants and most vibraitonal frequencies between our CC and Yu's CCSD(T)/cc-pVTZ[17] in the equlibrium structures is less than 5%. The calculated values of oxygen isotope fractionation by CC is higher than the other by around 0.5 per mil at low pressure and around 1 per mil at 1 atm. Thus, the structures and vibrational frequencies by CC is sufficiently good for the present study.

[45] Compared with the experimental result by Forney *et al.*,[56] the calculated vibrational frequencies in *trans*-HOCO. are larger by less than 5%, except for the OH stretching (6%).

Since the offset is small, no scaling factor of vibrational frequencies was used in calculating the number of states. However, to account approximately for the anharmonicity of the energetic intermediates, the density of states of *trans*- and *cis*-HOCO were increased by a constant factor, 1.5.[57] Again, this factor does not affect the low pressure fractionation.

[46] Recent high level *ab initio* calculations were used for the energies of stationary points in the LTSH potential.[23] Since the imaginary frequency of TS_2 in the LTSH potential is anomalously low, the vibrational frequencies and rotational constants of all stationary structures are calculated instead by *ab initio* methods. Only the energies without ZPE corrections of the stationary structures are obtained from the LTSH potential.

[47] The barrier heights of both TSs are robust with respective to the different calculations. Since the classical barrier of TS_1 at J=0 is lower than that of TS_2, and the structure of TS_2 is more compact than TS_1, the classical barrier of TS_1 is lower than TS_2 at all J. That is, there is no rotational channel switching[58] (change of principal exit channel with J).

[48] S. D. Chambreau, D. Townsend, S. A. Lahankar, S. K. Lee, and A. G. Suits, *Physica Scripta* **73**, C89 (2006).

[49] S. A. Lahankar, S. D. Chambreau, D. Townsend, F. Suits, J. Farnum, X. B. Zhang, J. M. Bowman, and A. G. Suits, *J Chem. Phys.* **125**, 044303 (2006).

[50] D. Townsend, S. A. Lahankar, S. K. Lee, S. D. Chambreau, A. G. Suits, X. Zhang, J. Rheinecker, L. B. Harding, and J. M. Bowman, *Science* **306**, 1158 (2004).

[51] The HO−CO distance of TS_1 optimized by B3LYP is too long, about 2.99 Å in B3LYP, so doubtful frequencies would be expected. A similar result happened when Lin used B3LYP/6-

311G(d,p) to calculate TS_1.[20] The calculated HO−CO distance of TS_1 calculated by CC and MP is 2.03 and 1.95 Å, respectively.

[52] Gaussian 98, Revision A.11.3, M. J. Frisch, G. W. Trucks, H. B. Schlegel, G. E. Scuseria, M. A. Robb, J. R. Cheeseman, V. G. Zakrzewski, J. A. Montgomery, Jr., R. E. Stratmann, J. C. Burant, S. Dapprich, J. M. Millam, A. D. Daniels, K. N. Kudin, M. C. Strain, O. Farkas, J. Tomasi, V. Barone, M. Cossi, R. Cammi, B. Mennucci, C. Pomelli, C. Adamo, S. Clifford, J. Ochterski, G. A. Petersson, P. Y. Ayala, Q. Cui, K. Morokuma, N. Rega, P. Salvador, J. J. Dannenberg, D. K. Malick, A. D. Rabuck, K. Raghavachari, J. B. Foresman, J. Cioslowski, J. V. Ortiz, A. G. Baboul, B. B. Stefanov, G. Liu, A. Liashenko, P. Piskorz, I. Komaromi, R. Gomperts, R. L. Martin, D. J. Fox, T. Keith, M. A. Al-Laham, C. Y. Peng, A. Nanayakkara, M. Challacombe, P. M. W. Gill, B. Johnson, W. Chen, M. W. Wong, J. L. Andres, C. Gonzalez, M. Head-Gordon, E. S. Replogle, and J. A. Pople, Gaussian, Inc, Pittsburgh PA, 2002.

[53] The equlibrium imaginary frequency of TS_2 is $1526i$, $2125i$, and $3176i$ for DFT, CC, and MP2, respectively.

[54] H. G. J. Smit, A. Volz, D. H. Ehhalt, and H. Knappe, in *Stable Isotopes*, edited by H. Schmidt, H. Förstel, and K. Heinzinger (Elsevier Scientific Publishing Company, 1982), pp. 147–152.

[55] C. M. Stevens, L. Kaplan, R. Gorse, S. Durkee, M. Compton, S. Cohen, and K. Bielling, *Int. J. Chem. Kinet.* **12**, 935 (1980).

[56] D. Forney, M. E. Jacox, and W. E. Thompson, *J. Chem. Phys.* **119**, 10814 (2003).

[57] J. Troe, *J. Chem. Phys.* **79**, 6017 (1983).

[58] J. Troe, *J Chem. Soc. Faraday Trans.* **90**, 2303 (1994).